Electromagnetic induction calibration using apparent electrical conductivity modelling based on electrical resistivity tomography

Article *in* Near Surface Geophysics · June 2010

DOI: 10.3997/1873-0604.2010037

CITATIONS
68

READS
516

10 authors, including:

François Lavoué
Université Grenoble Alpes
21 PUBLICATIONS **114** CITATIONS
SEE PROFILE

Jan Van der Kruk
Forschungszentrum Jülich
180 PUBLICATIONS **2,206** CITATIONS
SEE PROFILE

Frederic Andre
Université Catholique de Louvain - UCLouvain
63 PUBLICATIONS **906** CITATIONS
SEE PROFILE

Davood Moghadas
Brandenburg University of Technology Cottbus - Senftenberg
44 PUBLICATIONS **245** CITATIONS
SEE PROFILE

Near Surface Geophysics, 2010, **8**, 553-561 doi:10.3997/1873-0604.2010037

Electromagnetic induction calibration using apparent electrical conductivity modelling based on electrical resistivity tomography

F. Lavoué[1], J. van der Kruk[1*], J. Rings[1], F. André[1], D. Moghadas[1], J.A. Huisman[1], S. Lambot[1,2], L.Weihermüller[1], J. Vanderborght[1] and H. Vereecken[1]

[1] *Institute of Chemistry and Dynamics of the Geosphere, ICG-4 Agrosphere, Forschungszentrum Juelich, Gebaude 16.6, 52425 Juelich, Germany*

[2] *Earth and Life Institute, Université catholique de Louvain, 1, Place de l'Université, 1348 Louvain-la-Neuve, Belgium*

Received January 2010, revision accepted July 2010

ABSTRACT

Electromagnetic parameters of the subsurface such as electrical conductivity are of great interest for non-destructive determination of soil properties (e.g., clay content) or hydrologic state variables (e.g., soil water content). In the past decade, several non-invasive geophysical methods have been developed to measure subsurface parameters *in situ*. Among these methods, electromagnetic (EM) induction appears to be the most efficient one that is able to cover large areas in a short time. However, this method currently does not provide absolute values of electrical conductivity due to calibration problems, which hinders a quantitative analysis of the measurement. In this study, we propose to calibrate EM induction measurements with electrical conductivity values measured with electrical resistivity tomography (ERT). EM induction measures an apparent electrical conductivity at the surface, which represents a weighted average of the electrical conductivity distribution over a certain depth range, whereas ERT inversion can provide absolute values for local conductivities as a function of depth. EM induction and ERT measurements were collected along a 120-metre-long transect. To reconstruct the apparent electrical conductivity measured with EM induction, the inverted ERT data were used as input in an electromagnetic forward modelling tool for magnetic dipoles over a horizontally layered medium considering the frequencies and offsets used by the EM induction instruments. Comparison of the calculated and measured apparent electrical conductivities shows very similar trends but a shift in absolute values, which is attributed to system calibration problems. The observed shift can be corrected for by linear regression. This new calibration strategy for EM induction measurements now enables the quantitative mapping of electrical conductivity values over large areas.

INTRODUCTION

Water availability in the vadose zone controls important phenomena at different scales. At the catchment scale, near-surface soil moisture significantly influences infiltration, evaporation and runoff. At the field scale, water availability in the upper soil layers impact plants growth. At the local scale, soil water content has an effect on biological and chemical processes (e.g., CO_2 exchange between soil and atmosphere). Thus, understanding of the soil water distribution is an important issue in engineering, agricultural and environmental sciences and there clearly is a need for mapping soil water content at these different scales. In hydrogeophysics, soil water content is mapped at the regional scale with remote sensing techniques (e.g., radiometer, radar), whereas time domain reflectometry (TDR) is considered as the most accurate method to measure soil water content at the point scale (Rubin and Hubbard 2005; Robinson *et al.* 2008).

Nonetheless, many authors have pointed out the lack of a consistent method to measure soil water content at an intermediate scale (Pellerin and Wannamaker 2005; Abdu *et al.* 2007; Gebbers *et al.* 2009). One of the geophysical methods that could fill this gap at the field to headwater catchment scale is electromagnetic (EM) induction, which measures the apparent electrical conductivity of the soil. This method permits to cover large areas in a short time. Several authors have used EM induction to map soil water content (e.g., Kachanoski *et al.* 1988; Reedy and Scanlon 2003; Sherlock and McDonnell 2003; Abdu *et al.* 2008; Lück *et al.* 2009; Müller

* j.van.der.kruk@fz-juelich.de

et al. 2009). Typical source-receiver orientations to measure electrical conductivity are vertical magnetic dipoles or horizontal coplanar loops (HCP) and horizontal dipoles or vertical coplanar loops (VCP). These orientations have different depth sensitivity, which can be used to obtain electrical conductivity profiles with depth (e.g., Borchers *et al.* 1997; Hendrickx *et al.* 2002; Saey *et al.* 2009). Most studies use the sensitivity curves introduced by McNeill (1980) to model the cumulative response of the soil to the electromagnetic field generated by the instrument and to calculate its apparent electrical conductivity (Abdu *et al.* 2007; Callegary *et al.* 2007; Saey *et al.* 2009). However, these curves do not consider frequency dependency or angle-dependent reflection coefficients (Callegary *et al.* 2007). In addition, current EM induction systems return only qualitative values for electrical conductivity because of instrument calibration difficulties (Triantafilis *et al.* 2000; Sudduth *et al.* 2001; Abdu *et al.* 2007; Gebbers *et al.* 2009; Nüsch *et al.* 2010). Figure 1 shows repeated EM induction measurements with a GSSI Profiler EM induction system used at a frequency of 15 kHz in HCP orientation. The only difference between the three measured electrical conductivity profiles was that the system was recalibrated at the start of each profile measurement. All measurements were carried out within 15 minutes such that the observed static shift can only be due to the calibration and not to actual changes in the soil electrical conductivity. This clearly indicates that there is a need for an improved calibration of EM induction measurements that will enable a quantitative interpretation of electrical conductivity values. To overcome the limitations due to the lack of robust instrument calibration techniques and to avoid the simplifications that are commonly made with respect to electromagnetic wave propagation phenomena, Moghadas *et al.* (2010) introduced a new conceptual EM induction model adapted from the approach of Lambot *et al.* (2004) for ground-penetrating radar (GPR) for the particular case of zero-offset and off-ground EM induction configurations. It is important to note that this approach can currently not be applied to the widely used common-offset on-ground EM induction systems.

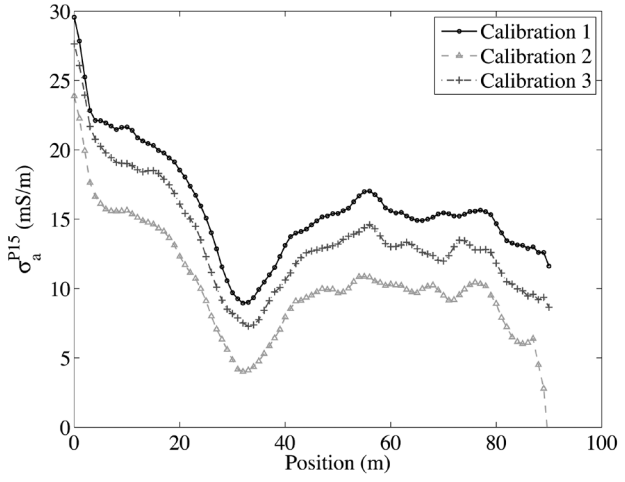

FIGURE 1
Repeated measurements with the Profiler at 15 kHz within a short time interval using a new calibration for each measurement.

In this study, an alternative calibration method is introduced that can be applied to common-offset on-ground EM induction systems. We propose to calibrate EM induction measurements using electrical conductivity values derived from electrical resistivity tomography (ERT) as input for an electromagnetic forward model that predicts the apparent electrical conductivity σ_a (S/m) measured with EM induction.

In the remainder of this paper, we first introduce the electromagnetic forward models, which are then used to develop the calibration method. Next, the test site, the measurement setup and the measured ERT and EM induction data are discussed. These ERT data are then used to predict apparent electrical conductivities measured with EM induction. The differences between measured and modelled apparent electrical conductivity values are corrected using a linear regression calibration, which results in calibrated electrical conductivity values derived from EM induction measurements.

APPARENT ELECTRICAL CONDUCTIVITY MODELS

In general, electrical conductivity values obtained using ERT and EM induction cannot be compared directly. Although both methods measure electrical conductivity values, ERT inversion returns lateral and vertical electrical conductivity values $\sigma(x,z)$, whereas EM induction returns values for an apparent electrical conductivity $\sigma_a(x)$ that reflects a cumulative electrical conductivity distribution over a certain depth range. Here, two approaches are discussed that can be used to calculate apparent electrical conductivity from ERT local electrical conductivity: the sensitivity curves described by McNeill (1980) and an electromagnetic forward model for a horizontally layered half-space that calculates the apparent conductivities measured with EM induction using less assumptions. Both methods are valid for horizontally layered media. In the following analysis, we neglect lateral variations and assume that measurements at each position can be approximated by measurements over a horizontally layered medium.

Local sensitivity curves

For a homogeneous half-space, McNeill (1980) introduced the relative responses (or local sensitivities) ϕ^{HCP} and ϕ^{VCP}, which correspond to the relative contribution of a thin layer at depth z to the secondary magnetic field generated by vertical and horizontal dipoles, respectively:

$$\phi^{HCP}(z,s) = \frac{4z/s}{(4(z/s)^2+1)^{3/2}}, \quad (1)$$

$$\phi^{VCP}(z,s) = 2 - \frac{4z/s}{(4(z/s)^2+1)^{1/2}}, \quad (2)$$

where z is the depth (m) and s is the distance between source and receiver (m). The apparent electrical conductivity $\sigma_a^{LS}(x,s)$ for HCP and VCP resulting from the ERT electrical conductivity $\sigma^{ERT}(x,z)$ is then

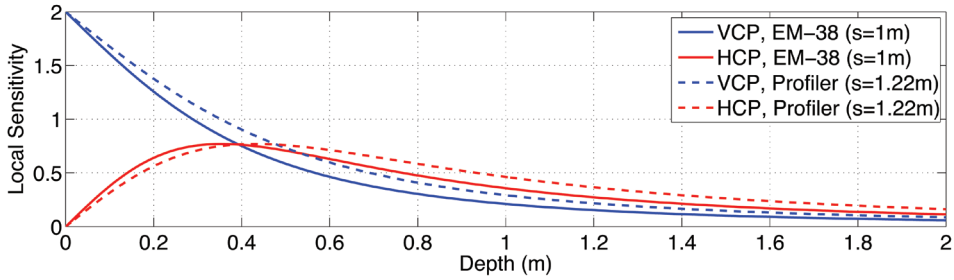

FIGURE 2
HCP and VCP local sensitivity curves for EM38 and Profiler.

$$\sigma_a^{LS}(x,s)=\frac{1}{s}\int_0^{\infty}\sigma^{ERT}(x,z)\phi^{\{HCP,VCP\}}(z,s)dz, \tag{3}$$

where the superscript *LS* stands for 'local sensitivity' and x (m) is the lateral position. To calculate the apparent electrical conductivity measured with EM induction, we must integrate the sensitivity over a depth range that is larger than the depth of the ERT profile (1.7 m). An integration up to z^{ERT} = 1.7 m would only consider 72% of the local-sensitivity-curves area. The contribution to the apparent electrical conductivity below the depth z^{ERT} is given by the cumulative responses $R^{\{HCP,VCP\}}$ (McNeill 1980):

$$R^{\{HCP,VCP\}}(z^{ERT},s)=\int_{z^{ERT}}^{\infty}\phi^{\{HCP,VCP\}}(z/s)dz, \tag{4}$$

hence,

$$R^{HCP}(z,s)=\frac{1}{\sqrt{4(z/s)^2+1}}, \tag{5}$$

and

$$R^{VCP}(z,s)=\frac{1}{\sqrt{4(z/s)^2+1}}-2z/s. \tag{6}$$

In our calculations, we assumed that the electrical conductivity below z^{ERT} is equal to the averaged electrical conductivity of the last two layers of the ERT profile. Using these expressions, the apparent conductivity for layered media can be calculated. It is important to note that equations (1)–(6) assume that the low induction number approximation is valid (Callegary *et al.* 2007). Figure 2 shows the sensitivity curves ϕ^{HCP} and ϕ^{VCP} for both modes and the two instruments used in this study (Geonics EM38 and GSSI Profiler). The HCP mode is more sensitive at depth (with a maximum of sensitivity at about 35 cm), whereas the VCP mode is more sensitive near the surface. The Profiler is slightly more sensitive at larger depths than the EM38 due to the larger distance between source and receiver (1.22 m versus 1.00 m). Note that these sensitivity curves do not include any frequency-dependency.

Electromagnetic forward model

The electromagnetic field for a horizontal and vertical dipole source-receiver combination over a horizontally layered earth can be written as (Ward and Hohmann 1987):

$$\sigma_a^{EM;HCP}(x,s)=\frac{-4s}{2\pi f\mu_0}\mathrm{Im}\left[\int_0^{\infty}R_0J_0(s\lambda)\lambda^2d\lambda\right], \tag{7}$$

$$\sigma_a^{EM;VCP}(x,s)=\frac{-4}{2\pi f\mu_0}\mathrm{Im}\left[\int_0^{\infty}R_0J_1(s\lambda)\lambda d\lambda\right], \tag{8}$$

where the reflection factor R_0 is obtained recursively beginning with the lowest layer $N+1$, where $R_{N+1}=0$,

$$R_n(h_n,\sigma_n)=\frac{\frac{\Gamma_n-\Gamma_{n+1}}{\Gamma_n+\Gamma_{n+1}}+R_{n+1}\exp(-2\Gamma_{n+1}h_{n+1})}{1+\frac{\Gamma_n-\Gamma_{n+1}}{\Gamma_n+\Gamma_{n+1}}R_{n+1}\exp(-2\Gamma_{n+1}h_{n+1})}, \tag{9}$$

$$\Gamma_n=\sqrt{\lambda^2+2\pi jf\mu_0\sigma^{ERT}(h_n)}, \tag{10}$$

$\sigma_0=0$, h_n is the height, $\sigma^{ERT}(h_n)$ is the ERT electrical conductivity for the n^{th} layer, J_0 and J_1 are the zeroth and first-order Bessel functions and λ is the radial wavenumber. Here, the relative contributions of electrical conductivity are less obvious. Compared to the local sensitivity curves of McNeill (1980) that are independent of frequency and use a low induction approximation, this electromagnetic forward model is exact and does not include any approximations. It includes the frequency dependency and the angle-dependent reflection coefficients between the different layers and their pertaining layer thicknesses. This model was also used by van der Kruk *et al.* (2000) who introduced an apparent conductivity concept that is not limited to the low-induction number approximation and renders a vertical conductivity distribution of the subsurface. We expect that this electromagnetic forward model returns more reliable apparent electrical conductivity values than the standard sensitivity curves, especially if high contrasts are present or in very conductive media where the low induction number approximation is not valid.

DESCRIPTION OF THE TEST SITE AND MEASUREMENT SETUP

The measurements were collected at a 180 m long and 60 m wide test site in Selhausen (North Rhine-Westphalia, Germany). Figure 3 shows the small topographical slope that varies between 0–4° from NE to SW. The surface soil contains up to 60% stones in weight in its upper part and 10% in the lower part. Soil samples were taken on a 10 m by 10 m raster (Bornemann *et al.* 2010) and show that the top soil (0–30 cm) contains 35% sand, 52% silt and 13% clay in the upper part of the field, compared to 13% sand, 70% silt and 17% clay in the lower part of the field (Fig. 4). Previous studies by Weihermüller *et al.* (2007) and Jadoon *et al.* (2010) using GPR, TDR and volumetric soil sam-

ples showed a gradient in soil water content from the upper to the lower part of the field, partly related to the changes in texture. We expect to find the effect of these trends in the electrical conductivity values measured along a representative 120-metre-long profile in the direction of the field slope.

Along the 120-metre-long transect on the test site, EM induction and ERT measurements were made. For ERT, we used a dipole-dipole configuration, which has a good vertical resolution and enabled us to take a large number of measurements using the multi-channel capability of the SYSCAL PRO system (IRIS Instruments, Orleans, France) with 120 electrodes. The spacing between electrodes was 25 cm and seven 30 m long profiles were measured using the roll-along technique with a 15 m overlap. The roll-along measurements were prepared so that no electrode configuration was measured twice. All measurements from the roll-along survey were combined into one large data set.

Along the ERT transect, EM induction measurements were conducted every metre with a Geonics EM38 system (frequency 14.5 kHz, source-receiver distance 1 m) and with a GSSI Profiler (frequencies 8 kHz and 15 kHz, source-receiver distance 1.22 m), both in HCP and VCP configurations. Both systems were calibrated by keeping the systems in the air and on the ground according to the specifications made by the manufacturer.

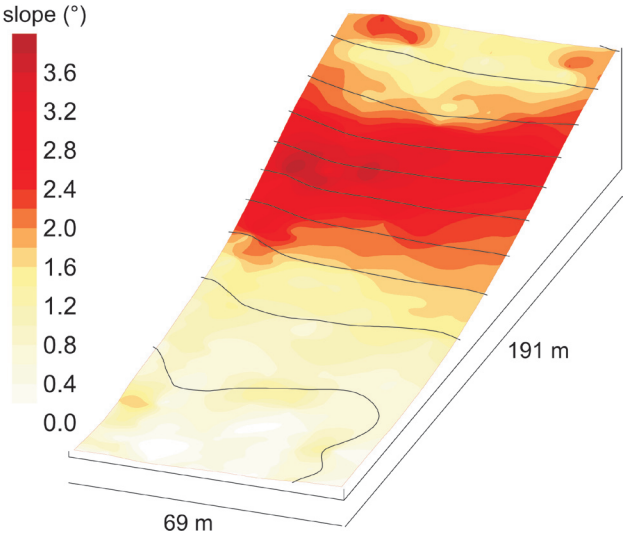

FIGURE 3
Topography and slope of the Selhausen test site.

EXPERIMENTAL RESULTS

ERT results

Erroneous values due to badly coupled electrodes or current injection problems during ERT measurements were removed. This resulted in a data set of 8391 measurements, which were inverted using the robust inversion method of the RES2DINV software (Loke *et al.* 2003) with the default damping parameters. The robust inversion scheme that uses the L1-norm for data and model space was used because we expected sharp layer boundaries. The inverted profile shown in Fig. 5 has an root mean square error of 1.01% and was obtained after 5 iterations. The final result was relatively independent of the starting model. The ERT inversion results provide values every 25 cm and with a variable separation with depth (data points are vertically located as black dots in Fig. 5). Values were then interpolated in the x-direction and selected at EM induction measurement locations (every metre).

The ERT profile in Fig. 5 clearly shows a lateral gradient of decreasing electrical conductivity for increasing distance, i.e., from the lower to the upper part of the field. These electrical conductivity changes can be related to soil water content changes and changes in texture, which were also observed by Weihermüller *et al.* (2007). In addition, the electrical conductivity increases with depth, which corresponds to an increase in water and/or clay content with depth. Two low electrical conductivity zones can also be observed between $25 < x < 55$ m and $80 < x < 92$ m,

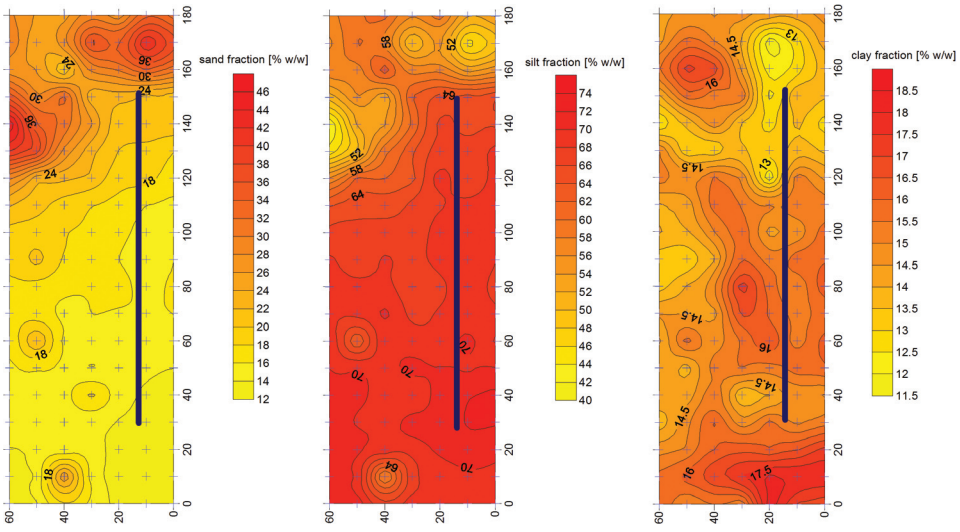

FIGURE 4
Sand, silt and clay fraction within the upper 30 cm obtained from sampling points on a 10 m raster indicated by the crosses. The 120-metre-long transect is indicated by the thick blue line.

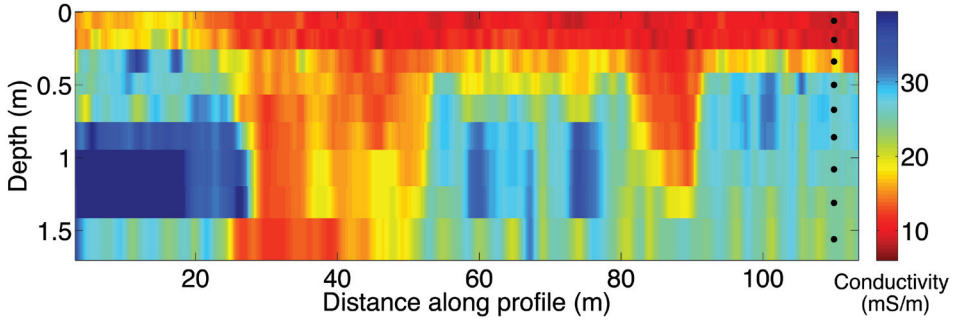

FIGURE 5
Vertical section of electrical conductivity along profile ($\sigma^{ERT}(x,z)$, mS/m) used for synthetic apparent conductivity calculations.

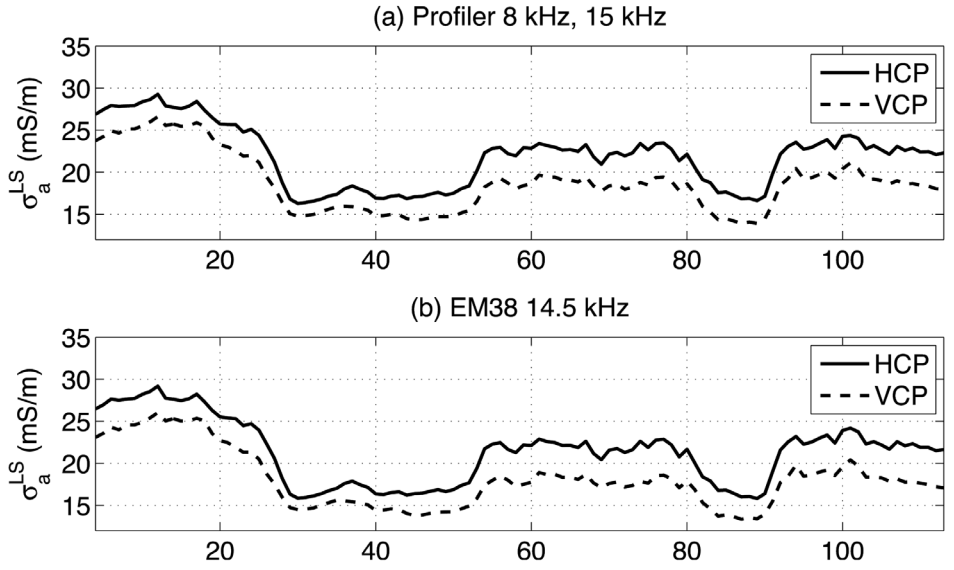

FIGURE 6
HCP and VCP apparent conductivities calculated using the ERT inversion results and the local sensitivity curves from McNeill (1980) for a) Profiler 8 kHz and 15 kHz and b) EM38 14.5 kHz.

with electrical conductivity values less than 20 mS/m at 1 m depth. These subsurface structures were not detected in any previous geophysical surveys (e.g., Weihermüller *et al.* 2007), because TDR and off-ground GPR measurements only sensed the upper few centimetres of soil and did not reach the depth of investigation of EM induction and ERT. These lateral and vertical electrical conductivity changes will be important features for the comparison and calibration of EM induction measurements using both HCP and VCP modes discussed later.

Apparent electrical conductivity calculations from ERT data and comparison with EM induction measurements

The local sensitivity curves shown in Fig. 2 suggest that HCP measurements will show a higher apparent electrical conductivity than VCP measurements for the soil electrical conductivity distribution shown in Fig. 5 because the electrical conductivity increases with depth. The Profiler is also expected to show a higher apparent electrical conductivity because it is more sensitive at depth than the EM38 due to its larger distance between source and receiver. In addition, the lower frequency (8 kHz) of the Profiler can result in a larger investigation depth and higher apparent electrical conductivity values. Finally, it is expected that the difference between the HCP and VCP modes should be less for a weak vertical gradient in electrical conductivity (for instance at $25 < x < 55$ m and $80 < x < 92$ m in Fig. 5). In the following, local sensitivity curves and electromagnetic forward modelling are used to calculate apparent electrical conductivity values using offset and frequency values used by the Profiler and EM38 systems.

Figure 6 shows modelled apparent electrical conductivity profiles over the 120-metre-long transect calculated with the sensitivity curves described in equations (1)–(6). Since the sensitivity curves do not depend on frequency, the modelled apparent electrical conductivity profiles do not differ for the 8 kHz and 15 kHz Profiler (Fig. 6a). The modelled apparent electrical conductivity values for the EM38 in Fig. 6(b) are slightly smaller than those of the Profiler due to the smaller offset between source and receiver.

Figure 7 shows modelled apparent electrical conductivity values calculated using the electromagnetic forward model (equations (7)–(10)) for the 8 kHz and 15 kHz Profiler and the EM38 configuration parameters. The HCP mode consistently results in larger apparent conductivities than the VCP mode, as expected from the ERT data presented in Fig. 5. In addition, the lower frequency (8 kHz) data show slightly higher electrical conductivity values than the higher frequency data (15 kHz) for the Profiler. As expected, the EM38 shows slightly smaller

apparent electrical conductivity values than the Profiler at 15 kHz due to its smaller offset between source and receiver. Moreover, in the areas with smaller vertical gradients ($25 < x < 55$ m and $80 < x < 92$ m in Fig. 5) the HCP and VCP conductivities are more similar than in other regions, which was expected from the sensitivity curves. In summary, the EM-based apparent electrical conductivity values are consistent with the ERT profile shown in Fig. 5 when considering dipole orientation (HCP or VCP), offset and frequency dependency.

Figure 8 compares the modelled data shown in Figs 6 and 7 with the measured EM induction data using the Profiler and EM38 systems. The EM-based apparent conductivities are similar to the measured values for the HCP configuration of the Profiler. However, a clear shift is present for all VCP modes and for the HCP mode of EM38. It also worth noting that the EM38 seems to be more sensitive to noise than the Profiler, especially in the HCP mode. To obtain quantitative measurements of apparent electrical conductivity using EM induction, the EM induction data can be calibrated using apparent conductivities calculated from ERT data. Since the EM-based modelling approach is based on the most accurate forward model, we will use this approach during calibration.

EM induction-ERT calibration

The measured apparent conductivities are plotted against the EM-based modelled apparent conductivities in Fig. 9 for the Profiler (8 kHz and 15 kHz) and EM38 in both the HCP and VCP configurations. In all cases, the HCP and VCP results do not match the 1:1 (dashed) line. This indicates the need for a calibration of EM induction measurements. As already observed in Fig. 8, all VCP measurements underestimate the EM-based apparent electrical conductivity. For Profiler measurements, HCP values agree well with modelled data, except for values corresponding to the low electrical conductivity zones, where the EM-based values are mostly smaller than the measurements. The EM38 data for a HCP configuration also seem to underestimate the apparent electrical conductivity values.

Three different calibrations were investigated, namely a shift, a scaling and a linear regression (which combines shifting and scaling). From comparing the improvement in error between calibrated and modelled values, it was decided that a linear regression was needed as it offers two degrees of freedom. The linear regression parameters were derived from the scatter plots in Fig. 9, where the resulting calibration curves are shown with dashed lines. The decrease in error due to calibration is listed in Table 1. Especially for the VCP configurations, the errors have been significantly reduced. These combined shift and scaling calibrations are applied to the measured apparent electrical con-

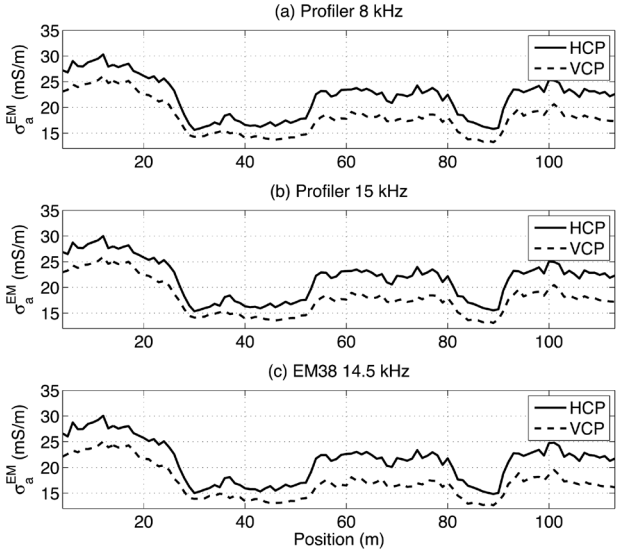

FIGURE 7

HCP and VCP apparent conductivities calculated using the ERT inversion results and electromagnetic forward modelling for a) Profiler 8 kHz, b) Profiler 15 kHz and c) EM38 14.5 kHz.

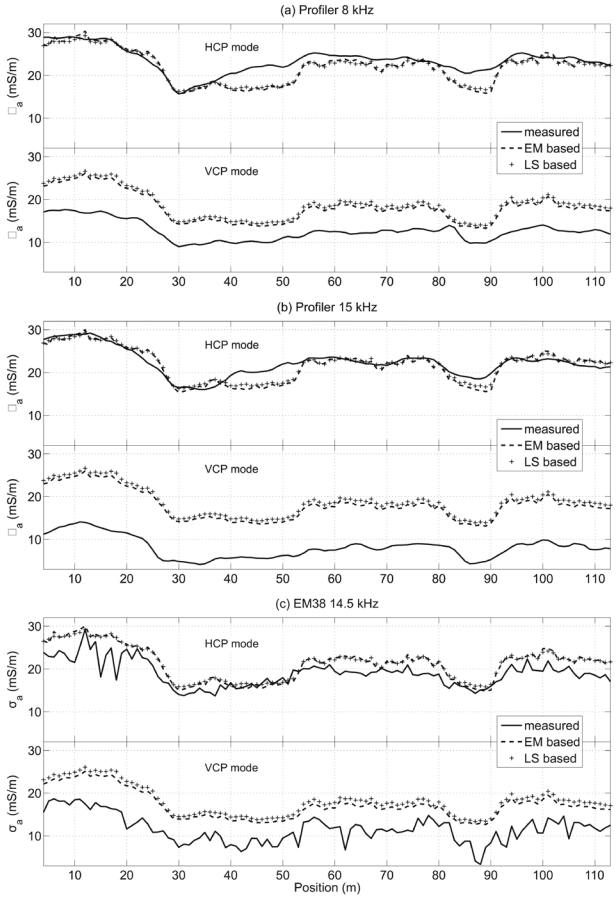

FIGURE 8

HCP and VCP apparent conductivity profiles for a) Profiler 8 kHz, b) Profiler 15 kHz and c) EM38 from EM induction measurements, calculation based on the electromagnetic forward model and calculation using the sensitivity curves.

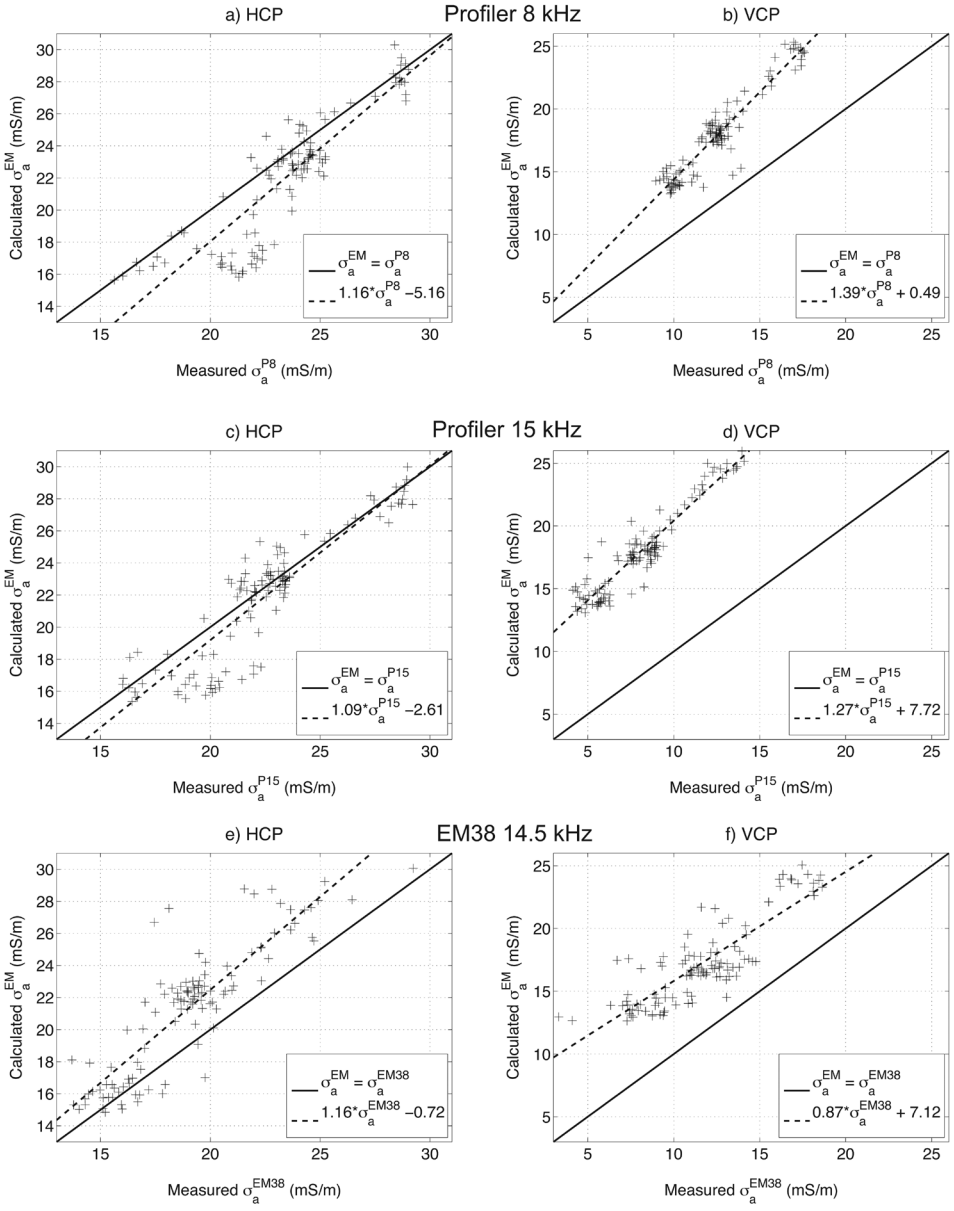

FIGURE 9
HCP and VCP scatter plots of measured $\sigma_a^{\{P8,\ P15,\ EM38\}}$ versus EM-based σ_a^{EM} for Profiler 8 (a, b) and 15 (c, d) KHz and EM38 (e, f), respectively. Dashed lines show the corresponding linear regressions.

ductivity data and compared to the modelled EM-based data in Fig. 10. After calibration, the variations of the electrical conductivity along the transect for the measured and modelled data agree very well, except for $25 < x < 55$ m. This discrepancy could be due to 3D effects, which will be investigated in the future.

Although we believe that the results presented here are promising, there are several critical issues. First, the current results are based on a horizontally layered medium and the effects of laterally varying conductivity are ignored. Second, we compare ERT electrical conductivity values measured using a frequency of 2 Hz with EM induction data measured at higher frequencies. Therefore, our approach assumes a frequency independent electrical conductivity in this frequency range. Finally, ERT and EM induction rely on different coupling mechanisms (i.e., galvanic and inductive, respectively). Nevertheless, the good match between measured and modelled EM induction data after calibration is promising and warrants further investigation.

CONCLUSIONS

ERT and EM induction measurements were carried out on a test site with moderate lateral and vertical variation in electrical conductivity. A comparison of the measured EM induction apparent conductivities with modelled apparent conductivities calculated from ERT conductivities showed that the trends are very similar. However, a clear shift was present for the measured EM induction data, such that the EM induction values cannot be quantitatively interpreted directly. Using modelled apparent conductivities obtained from an electromagnetic forward model, the EM

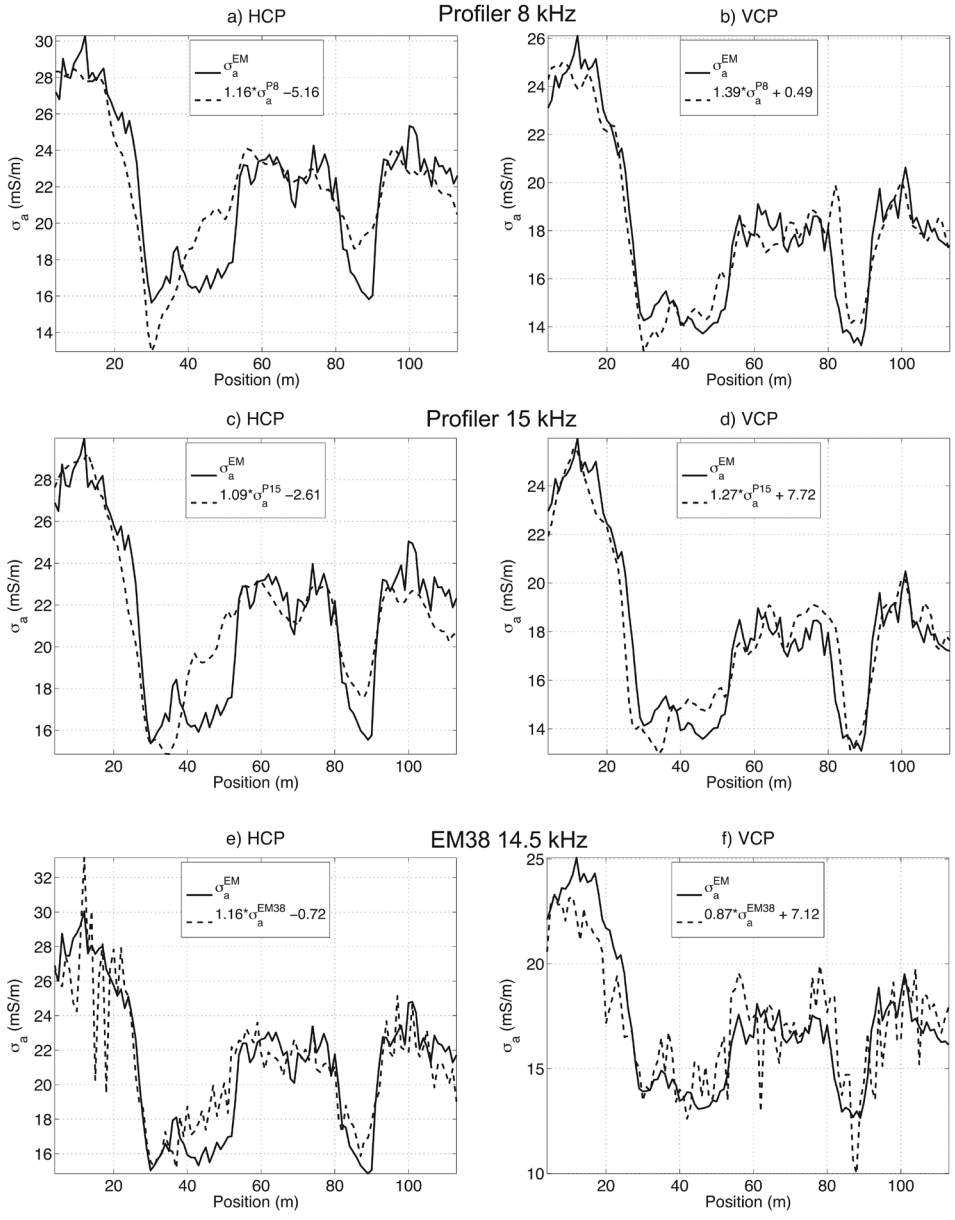

FIGURE 10
HCP and VCP EM-based calculated apparent conductivities (black) and calibrated values from measured apparent conductivities (dashed line) for Profiler 8 (a, b) and 15 (c, d) kHz and EM38 (e, f), respectively.

TABLE 1
Absolute errors between measured and calculated conductivity values (in mS/m)

	Mode	Mean error for original values	Mean error for calibrated values	Linear regression curves
Profiler 8 kHz	HCP	1.7493	1.4822	$1.16\sigma_a^{P8} - 5.16$
	VCP	5.4663	0.8215	$1.39\sigma_a^{P8} + 0.49$
Profiler 15 kHz	HCP	1.3499	1.3398	$1.09\sigma_a^{P15} - 2.61$
	VCP	9.8673	0.8769	$1.27\sigma_a^{P15} + 7.72$
EM38	HCP	2.5092	1.4291	$1.16\sigma_a^{EM38} - 0.72$
	VCP	5.5766	1.3991	$0.87\sigma_a^{EM38} + 7.12$

induction measurements were calibrated using the ERT data. After calibration, the variations in measured and modelled apparent electrical conductivity match very well. Reliable quantitative values are vital for making a multi-layered inversion using HCP and VCP measurements possible. Any static shift will have a dramatic influence on the inversion results. Having quantitative EM induction values and the possibility of acquiring EM induction data on large-scales offers great potential for a wide range of applications. Nevertheless, more measurements at different sites must be performed to investigate the reliability of the calibration approach proposed here. The extension of the calibration approach for media with strong lateral variations in electrical conductivity is future work.

ACKNOWLEDGEMENTS

We acknowledge the support by the SFB/TR 32 'Pattern in Soil-Vegetation-Atmosphere Systems: Monitoring, Modelling and Data Assimilation' funded by the Deutsche Forschungsgemeinschaft (DFG). This project was initiated during a three-month internship of F. Lavoué at the Forschungszentrum Juelich. F. Lavoué acknowledges the support of the École Normale Supérieure de Lyon, France. Two anonymous reviewers helped to improve the manuscript.

REFERENCES

Abdu H., Robinson D.A. and. Jones S.B. 2007. Comparing bulk soil electrical conductivity determination using the DUALEM-1S and EM38-DD electromagnetic induction instruments. *Soil Science Society of America Journal* **71,** 189–196. doi:10.2136/sssaj2005.0394

Abdu H., Robinson D.A., Seyfried M. and Jones S.B. 2008. Geophysical imaging of watershed subsurface patterns and prediction of soil texture and water holding capacity. *Water Resources Research* **44**, W00D18. doi:10.1029/2008WR007043

Borchers B., Uram T. and Hendrickx J.M.H. 1997. Tikhonov regularization of electrical conductivity depth profiles in field soils. *Soil Science Society of America Journal* **61**, 1004–1009.

Bornemann L., Welp G. and Amelung W. 2010. Particulate organic matter at the field scale: Rapid acquisition using mid-infrared spectroscopy. *Soil Science Society of America Journal* **74**, 1147–1156.

Callegary J.B., Ferre T.P.A. and Groom R.W. 2007. Vertical spatial sensitivity and exploration depth of low-induction-number electromagnetic-induction instruments. *Vadose Zone Journal* **6,** 158–167. doi:10.2136/vzj2006.0120

Gebbers R., Lück E., Dabas M. and Domsch H. 2009. Comparison of instruments for geoelectrical soil mapping at the field scale. *Near Surface Geophysics* **7**, 179–190. doi:10.3997/1873-0604.2009011

Hendrickx J.M.H., Borchers B., Corwin D.L., Lesch S.M., Hilgendorf A.C. and Schlue J. 2002. Inversion of soil conductivity profiles from electromagnetic induction measurements: Theory and experimental verification. *Soil Science Society of America Journal* **66**, 673–685.

Jadoon K.Z., Lambot S., Scharnagl B., van der Kruk J., Slob E. and Vereecken H. 2010. Quantifying field-scale surface soil water content from proximal GPR signal inversion in the time domain. *Near Surface Geophysics* **8**, 483–491.

Kachanoski R.G., Gregorich E.G. and Vanwesenbeeck I.J. 1988. Estimating spatial 365 variations of soil-water content using noncontacting electromagnetic inductive methods. *Canadian Journal of Soil Science* **68**, 715–722.

van der Kruk J., Meekes J.A.C., van den Berg P.M. and Fokkema J.T. 2000. An apparent-resistivity concept for low-frequency electromagnetic sounding techniques. *Geophysical Prospecting* **48**, 1033–1052.

Lambot S., Slob E.C., van den Bosch I., Stockbroeckx B. and Vanclooster M. 2004. Modeling of ground-penetrating radar for accurate characterization of subsurface electric properties. *IEEE Transactions on Geoscience and Remote Sensing* **42**, 2555–2568.

Loke M.H., Acworth I. and Dahlin T. 2003. A comparison of smooth and blocky inversion methods in 2D electrical imaging surveys. *Exploration Geophysics* **34**, 182–187.

Lück E., Gebbers R., Ruehlmann J and Spangenberg U. 2009. Electrical conductivity mapping for precision farming. *Near Surface Geophysics* **7**, 15–26.

McNeill J.D. 1980. Electromagnetic terrain conductivity measurements at low induction numbers. Geonics Technical Note TN-6.

Moghadas D., André F., Vereecken H. and Lambot S. 2010. Efficient loop antenna modeling for zero-offset, off-ground electromagnetic induction in multilayered media. *Geophysics* (in press).

Müller M., Kurz G. and Yaramanci U. 2009. Influence of tillage methods on soil water content and geophyscial properties. *Near Surface Geophysics* **7**, 27–36.

Nüsch A., Dietrich. P., Werban U. and Behrens T. Acquisition and reliability of geophysical data in soil science. 19th World Congress of Soil Science, 1–6 August, Brisbane, Australia, Expanded Abstracts.

Pellerin L. and Wannamaker P.W. 2005. Multi-dimensional electromagnetic modeling and inversion with application to near-surface earth investigations. *Computers and Electronics in Agriculture* **46**, 71–102.

Reedy R.C. and Scanlon B.R. 2003. Soil water content monitoring using electromagnetic induction. *Journal of Geotechnical and Geoenvironmental Engineering* **129**, 1028–1039.

Robinson D.A., Binley A., Crook N., Day-Lewis F.D., Ferré T.P.A., Grauch V.J.S., Knight R., Knoll M., Lakshmi V., Miller R., Nyquist J., Pellerin L., Singha K. and Slater L. 2008. Advancing process-based watershed hydrological research using near-surface geophysics: A vision for and review of, electrical and magnetic geophysical methods. *Hydrological Processes* **22**, 3604–3635.

Rubin Y. and Hubbard S.S. 2005. *Hydrogeophysics*. Springer.

Saey T., Simpson D., Vermeersch H., Cockx L. and Van Meirvenne M. 2009. Comparing the EM38DD and DUALEM-21S sensors for depth-to-clay mapping. *Soil Science Society of America Journal* **73,** 7–12. doi:10.2136/sssaj2008.0079

Sherlock M.D. and McDonnell J.J. 2003. A new tool for hillslope hydrologists, spatially distributed groundwater level and soil water content measured using electromagnetic induction. *Hydrological Processes* **17**, 1965–1977.

Sudduth K.A., Drummond S.T. and Kitchen N.R. 2001. Accuracy issues in electromagnetic sensing of soil electrical conductivity for precision agriculture. *Computers and Electronics in Agriculture* **31**, 239–264.

Triantafilis J., Laslett G.M. and McBratney A.B. 2000. Calibrating an electromagnetic induction instrument to measure salinity in soil under irrigated cotton. *Soil Science Society of America Journal* **64**, 1009–1017.

Ward S.H. and Hohmann G.W. 1987. Electromagnetic theory for geophysical applications. In: *Electromagnetic Methods in Applied Geophysics, Vol. 1: Theory* (ed. M.N. Nabighian), pp. 130–311. SEG.

Weihermüller L., Huisman J.A., Lambot S., Herbst M. and Vereecken H. 2007. Mapping the spatial variation of soil water content at the field scale with different ground penetrating radar techniques. *Journal of Hydrology* **340**, 205–216.